Available online at www.sciencedirect.com
ScienceDirect
Sensors and Actuators A 145–146 (2008) 423–429
SENSORS AND ACTUATORS A PHYSICAL
www.elsevier.com/locate/sna

Design and fabrication of MEMS thermoelectric generators with high temperature efficiency

Till Huesgen *, Peter Woias, Norbert Kockmann

Laboratory for Design of Microsystems, Department of Microsystems Engineering-IMTEK, University of Freiburg, Georges-Koehler-Allee 102, D-79110 Freiburg, Germany

Received 28 June 2007; received in revised form 2 October 2007; accepted 29 November 2007
Available online 5 December 2007

Abstract

For MEMS devices with power consumption in the range of micro-watts, thermal energy harvesting becomes a viable candidate for power supply. This paper describes a multipurpose platform to fabricate thermoelectric generators in a combined surface and bulk micromachining process. The thermocouples are deposited by thin-film processes with high integration density on the wafer surface. To provide a large thermal contact area, the heat flow path is perpendicular to the chip surface (cross-plane) and guided by thermal connectors. One thermocouple junction is thermally connected via electroplated metal stripes to the heat source and thermally insulated to the heat sink by a cavity in the wafer substrate. Simulations show that approximately 95% of the entire temperature difference over the device is located between the two thermocouple junctions. Power factors of $3.63 \times 10^{-3}\ \mu W\,mm^{-2}\,K^{-2}$ and $8.14 \times 10^{-3}\ \mu W\,mm^{-2}\,K^{-2}$ can be achieved with thermopiles made of Al and n-poly-Si or p-$Bi_{0.5}Sb_{1.5}Te_3$ and n-$Bi_{0.87}Sb_{0.13}$, respectively. Measurements of fabricated devices show a linear output voltage of $76.08\ \mu V\,K^{-1}$ per thermocouple and prove the feasibility of the concept.

Keywords: Energy harvesting; Thermoelectric generator; Thermopiles; Seebeck effect

1. Introduction

In thermoelectric generators, the Seebeck effect is used for the direct conversion of a temperature difference into an electric potential between a material pair junction, the thermocouple. Already in 1958 it was proposed to power radio receivers in remote areas with thermoelectric generators using the waste heat of a petroleum lamp [1]. Also deep space missions like "Voyager" are supplied with electric energy from radioisotope thermoelectric generators (RTGs) [2]. More recently, micro-fabricated thermoelectric generators (μ-TEGs) have been used to power wrist-watches by heat released from the human body [3].

The miniaturization of thermoelectric devices is very promising because a high number of material pairs can be integrated into a small device, which results in high voltages already at small temperature differences. One approach to achieve this integration is to scale down "macroscopic" Peltier coolers. Vertical thermopiles, fabricated by means of thick-film technology, are connected electrically in series and sandwiched thermally in parallel between two substrates. An example is generators and Peltier coolers on the base of BiTe alloys, which are commercially available in microminiaturized versions [4]. In the production process of these elements, each of the two materials is sputtered in 20 μm thick layers onto a silicon wafer, individually structured by reactive ion etching, and then combined by bonding. On a chip size of 1.12 mm^2, 12 thermocouples are integrated and deliver an output power of 67 μW at a temperature difference of 5 K. A similar device with electrochemically deposited BiTe compounds has been developed by the Jet Propulsion Laboratory at CalTec [5]. At the ETH Zürich, flexible polymer-based generators with thermocouples made of electroplated Cu and Ni or BiTe-based alloys are investigated [6].

An alternative approach to miniaturize thermoelectric generators are membrane-based thin-film thermopiles, which are widely used for different sensor applications such as the measurement of IR radiation, vacuum, gas flow, or heat flux [7]. This technology has first been adapted by HSG-IMIT and Kundo [8].

* Corresponding author. Tel.: +49 761 203 7584; fax: +49 761 203 7492.
E-mail address: huesgen@imtek.de (T. Huesgen).

0924-4247/$ – see front matter © 2007 Elsevier B.V. All rights reserved.
doi:10.1016/j.sna.2007.11.032

Thermopiles, made of n-doped mono-Si and Al, are integrated into a Si membrane. However, drawbacks are a high parasitic heat flux through the membrane and difficulties in applying an in-plane temperature difference to the chip-like device. Infineon has developed generators with thermocouples made of poly-Si or poly-SiGe in BiCMOS technology [9]. These generators have in-plane thermopiles but a cross-plane heat flow, to allow thermal contacting via the large top and bottom footprint areas of the device. Therefore, a cavity is introduced into the substrate. Yet, thermal insulation on the front side of the device seems to be insufficient, limiting the effective temperature difference between the thermocouple junctions. A similar device with improved thermal insulation was recently presented in [10].

This paper describes the design and fabrication of a thermoelectric generator with optimized heat flow path, so that a maximum temperature difference is located between the thermocouple junctions. The meandering thermocouples (n-poly-Si/Al) are located on a Si wafer and are fabricated in thin-film technology to achieve a high integration density. The modular fabrication process also offers the opportunity to employ other materials, such as BiTe alloys, or self-organized superlattice materials, that provide superior thermoelectric properties [11]. The heat flux is guided perpendicular to the substrate plane to the planar thermocouple junctions by metal stripes with high thermal conductivity. Hence, the heat flux from the ambient area is introduced vertically over the footprint area of the chip, guided through the thermocouples in a planar direction, and released vertically over the footprint area. This arrangement guarantees a maximum thermal coupling of the generator to the environment and a maximum temperature gradient over the thermocouples. Due to direct correlation between the electrical current and the heat flux across the device, the proposed setup can also be used as sensor for a direct measurement of heat flux or a temperature difference. The fabricated devices are tested and compared with simulation results. Experimental thermoelectric properties and device characteristics are compared with literature data.

2. Fundamentals of thermoelectric energy conversion

The thermoelectric effect describes the coupling between electric and thermal currents, such as the occurrence of an electric voltage due to a temperature difference between two material contacts, the Seebeck effect. In reverse, an electrical current can produce a heat flux or a cooling of a material contact, called Peltier effect. A third effect is also connected with thermoelectricity, the Thomson effect, where an electric current flowing along a temperature gradient can absorb or release heat from or to the environment [2]. The relation between the first two mentioned effects can be described by methods of irreversible thermodynamics and the linear transport theory of Onsager in vector form.

$$\begin{bmatrix} q_{\mathrm{el}} \\ \dfrac{q_{\mathrm{th}}}{T} \end{bmatrix} = \begin{bmatrix} \sigma_{\mathrm{el}} & L_{\mathrm{S}} \\ L_{\mathrm{P}} & L_{\mathrm{q}} \end{bmatrix} \begin{bmatrix} \Delta U \\ \Delta T \end{bmatrix} \tag{1}$$

The specific electric current density q_{el} and the thermal entropy flux q_{th}/T are linked to the driving forces, the temperature gradient ΔT, and the potential gradient ΔU with linear coefficients L_{q} for the heat transfer, L_{S} for the Seebeck effect, and L_{P} for the Peltier effect. The derivation of the coefficients here follows the notation of Nolas et al. [12], another good description is given by Kalitzin [13].

Solving the first equation for ΔU and substituting the result into the following equation yields:

$$\begin{aligned} -\Delta U &= \frac{q_{\mathrm{el}}}{\sigma_{\mathrm{el}}} + \frac{L_{\mathrm{S}}}{\sigma_{\mathrm{el}}}\Delta T \\ q_{\mathrm{th}} &= T\frac{L_{\mathrm{P}}}{\sigma_{\mathrm{el}}} q_{\mathrm{el}} + T\left(\frac{L_{\mathrm{S}}L_{\mathrm{P}}}{\sigma_{\mathrm{el}}} - L_{\mathrm{q}}\right)\Delta T \end{aligned} \tag{2}$$

The matrix in the above equation is symmetric according to the Onsager reciprocity law [14] which means $L_{\mathrm{S}} = L_{\mathrm{P}}$. The linear coefficients can be identified with known material properties

$$\begin{aligned} \rho_{\mathrm{el}} &= \frac{1}{\sigma_{\mathrm{el}}} \\ \lambda_{\mathrm{th}} &= -T\left(\frac{L_{\mathrm{S}}L_{\mathrm{P}}}{\sigma_{\mathrm{el}}} - L_{\mathrm{q}}\right) = -T\left(\frac{L_{\mathrm{S}}^2}{\sigma_{\mathrm{el}}} - L_{\mathrm{q}}\right) \\ \alpha_{\mathrm{ab}} &= \frac{L_{\mathrm{S}}}{\sigma_{\mathrm{el}}} \\ \pi_{\mathrm{ab}} &= T\frac{L_{\mathrm{P}}}{\sigma_{\mathrm{el}}} \end{aligned} \tag{3}$$

The thermoelectric temperature measurement employs the Seebeck effect, the voltage between two material pair contacts on a different temperature level without the flow of electrical current ($Q_{\mathrm{el}} = 0$). The Seebeck effect is also described with the correlation

$$\Delta U = (\alpha_{\mathrm{a}} - \alpha_{\mathrm{b}})\,\Delta T = \alpha_{\mathrm{ab}}\Delta T \tag{4}$$

with the Seebeck coefficient α_{ab} with unit (V/K) for the material pair a–b. The Seebeck coefficient depends on the material pair and is often expressed by only one coefficient α. Certain applications, such as temperature measurement or energy conversion, demand for certain material properties like electric or thermal conductivity or temperature linearity. For temperature measurement, standardized elements and material pairs are used with good linearity of the material properties, reproducibility, and long-term stability. Thermoelectric energy conversion demands for high efficiency of the material such as BiTe alloys or superlattice structures [11]. These materials are designed for low thermal conductivity to provide a high temperature gradient between the thermocouple junctions. The material effectiveness for energy conversion is expressed by the figure-of-merit Z

$$Z = \frac{\alpha^2}{\rho\lambda} \tag{5}$$

which includes the electric and thermal conductivity of the material, ρ and λ, respectively. The conversion efficiency of a thermocouple is not only depending on the material properties, but also on the geometric cross-sectional areas of the

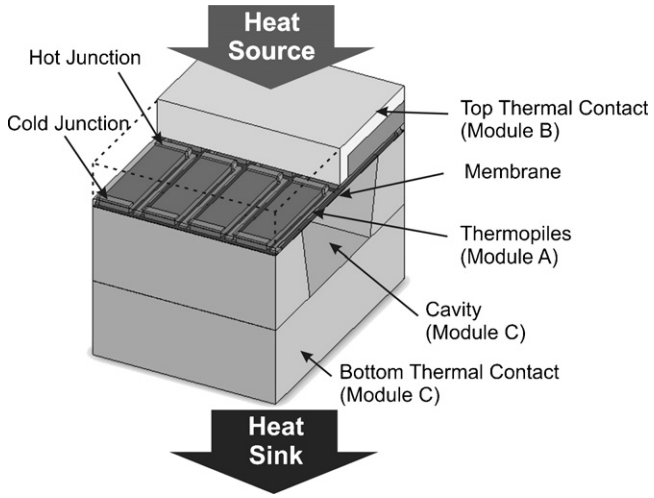

Fig. 1. Schematic of the microstructured thermoelectric generator with optimized heat flow path. The prototype is fabricated with thermopiles made of n-poly-Si and Al.

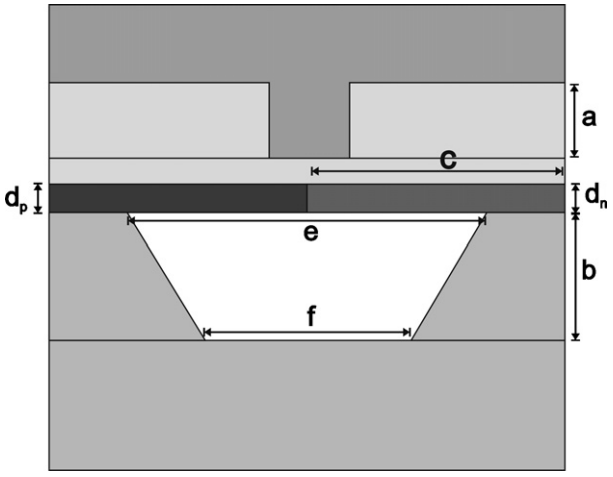

Fig. 2. Simplified schematic cross-section of the device indicating the key geometric parameters: (a) insulation layer thickness, (b) substrate thickness, (c) thermopile length, ($d_{n,p}$) n-, p-type thermopile thickness, (e) membrane length, and (f) mask opening for backside DRIE. Note that the thermopile thickness can be different for the two thermoelectric materials.

thermocouple legs. The optimum is found for [12]:

$$\frac{A_n}{A_p} = \sqrt{\frac{\lambda_p \rho_n}{\lambda_n \rho_p}} \tag{6}$$

with A_n and A_p being the geometric cross-section of the n-type and p-type thermocouple leg, respectively.

To increase the thermoelectric voltage, thermocouples are electrically connected in series, leading to a meandering structure between the hot and cold side of the device. The maximum electric power of a meandering thermocouple structure with n pairs in series is given by

$$P_{el} = \frac{n^2 \alpha^2 \Delta T^2}{4 R_i} \tag{7}$$

with the temperature difference ΔT between hot and cold junction and the internal electric resistance R_i. The device power factor p of a device expresses the electric energy yield for a certain temperature difference and device area A, where the heat is absorbed.

$$p = \frac{P_{el}}{\Delta T^2 A} \tag{8}$$

This value is used to compare the effectiveness of different devices.

3. Design and modeling

Due to the combined in-plane and cross-plane structure of the device, the design and fabrication are segmented into three modules, see Fig. 1. Module A concerns the thermoelectric structure on a substrate, basically, a rectangular meander made of the thermocouple materials deposited on a Si wafer. A barrier layer of SiO_2 insulates the thermopiles to prevent electrical short-circuit by the thermal contact structure fabricated in Module B. This concept allows to employ all kinds of thermoelectric materials that can be deposited on a Si substrate. For a functional prototype, n-doped poly-Si and Al are chosen in this work, due to their availability in the in-house clean-room facilities. Module B describes the thermal connectors on top of the thermoelectric structure to conduct the heat from the top surface to the hot thermocouple junction. For this purpose, metal is deposited within trenches formed by thermally insulating SU-8 photoresist. The large area on top serves as thermal contact pad for the device. In Module C, the hot junction is thermally insulated from the substrate by a backside DRIE process through the substrate, such that the cold junction is thermally connected with the bottom, cold side of the generator. A second wafer is bonded to the backside to realize a good thermal contact and to avoid cavity contamination.

The geometric properties are determined by physical and technological constraints. Therefore, experimental investigations and theoretical considerations are performed to find the

Table 1
Thermoelectric material data used in the FEM simulations

Material	Seebeck coefficient α ($\mu V K^{-1}$)	Electrical resistance ρ ($\mu\Omega$ m)	Thermal conductivity λ ($W m^{-1} K^{-1}$)	Reference
Aluminum	−1.7	0.043[a]	237	[15]
n-poly-Si	−107.88[a]	6.294[a]	37.3	[15]
p-$Bi_{0.5}Sb_{1.5}Te_3$	−100	17.25	1.05	[7]
n-$Bi_{0.87}Sb_{0.13}$	230	7.15	3.10	[7]

[a] Data obtained by measurements performed within this work.

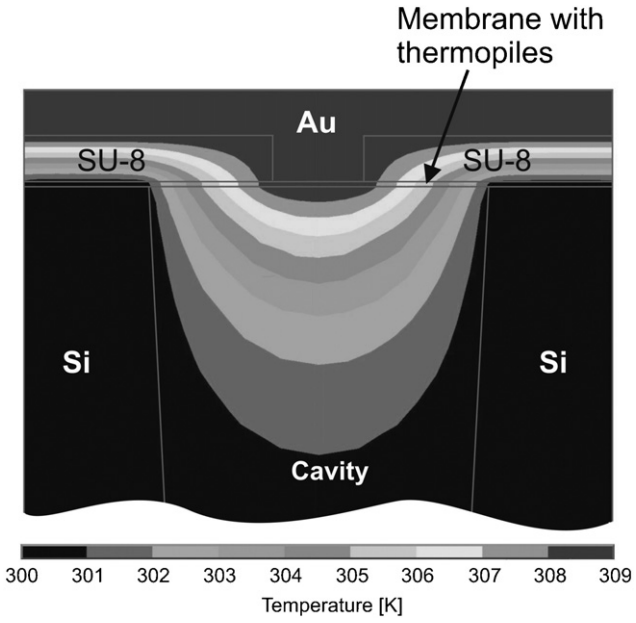

Fig. 3. Temperature profile over the μ-TEG with a total temperature difference of 9 K, resulting in 8.43 K between the thermocouple junctions.

key geometric parameters of the generator as shown in Fig. 2. To compensate for the higher thermal and electrical conductivity of Al compared to poly-Si, the ratio of the thermocouples cross-sectional area is determined with respect to Eq. (6). With the material properties given in Table 1 an optimum ratio $A_n/A_p = 30.5$ is calculated. Due to the slow deposition rate, a poly-Si layer thickness of 700 nm is chosen. As the aluminum is deposited on top, a layer thickness of 250 nm is necessary for sufficient step coverage. A poly-Si leg width of 40 μm and an Al leg width of 5 μm results in a cross-section ratio of $A_n/A_p = 22.4$, which is close to the optimum value. Each thermopile has a length of 120 μm.

In order to determine the possible layer thickness of the insulating polymer resist on the front side (Module B) experiments are carried out. Crack free layers of SU-8-2010 can be realized up to a thickness of 20 μm without adhesion problems. For the fabrication of the cavity (Module C), two opposing aspects have to be considered: the membrane length has to be maximized while at the same time the mask opening has to be minimized to leave sufficient footprint area for the bonding of the second wafer. Therefore, a deep reactive ion etching process that yields negative side walls, is developed. Due to backscattering of ions, over etching leads to notches that further increase the membrane length. A membrane length of 180 μm is achieved with a mask opening of 120 μm.

A 2D model as shown in Fig. 3 is used for thermal FEM simulations with ANSYS. To determine the performance benchmarks, a prototype generator with a total number of 7500 thermopiles (120 μm long) on a chip size of 10 mm × 10 mm is modeled. The thermoelectric material properties used for the simulation are given in Table 1. A temperature difference of 10 K across the entire chip yields an open-circuit voltage of 7.46 V and a maximum output power of 36.3 μW. The effective temperature difference between the thermocouple junctions is determined to 9.37 K. Furthermore, the simulation allows to calculate the thermal resistance of the device which is 1.555 K W^{-1}.

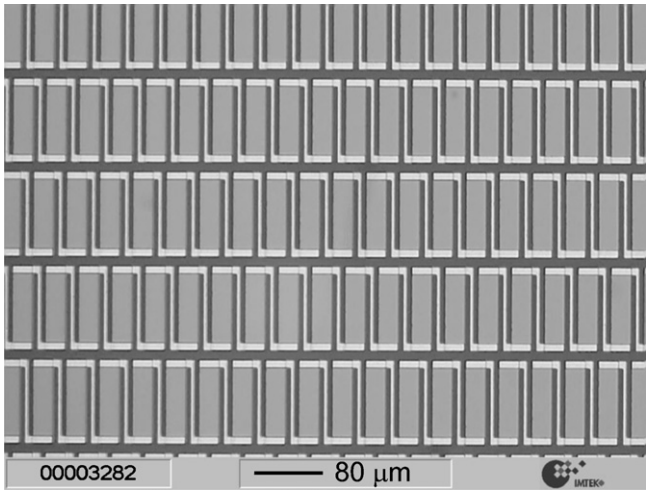

Fig. 4. Microscope image of the thermocouple meander after Al wet etch.

A thermoelectric generator with similar geometric parameters, but thermocouples made of p-$Bi_{0.5}Sb_{1.5}Te_3$ and n-$Bi_{0.87}Sb_{0.13}$, is also investigated in the simulation. Considering the thermoelectric material properties, the ratio of cross-sections is changed to $A_n/A_p = 0.375$ by adapting the thermopile width and height. All other geometric properties are maintained. The effective temperature difference is 9.58 K with 10 K applied across the device. This yields an open-circuit voltage of 23.8 V and a maximum output power of 81.4 μW. The thermal resistance is 2.127 K W^{-1} for this device. To compare these results with other devices, the device power factors are calculated according to Eq. (7) and are summarized in Table 2.

4. Fabrication

For the fabrication of the thermocouple structures (Module A), a 300 μm thick 4-in. silicon wafer serves as substrate. Thermal SiO_2 and LPCVD Si_3Ni_4 (each 300 nm thick) are subsequently deposited onto the wafer for electrical insulation and serve as supporting membrane. In situ n-doped poly-Si is deposited and structured by dry etching. The remaining poly-Si bars are covered with a 250 nm thick sputtered Al layer that is wet etched to form the meandering thermocouple structure (see

Table 2
Simulated performance benchmarks of thermoelectric generators with 7500 thermocouples, 120 μm long on a chip with a footprint area of 100 mm^2

Material pair	Temperature efficiency (%)	Open-circuit voltage/area (mV mm^{-2} K^{-1})	Device power factor (μW mm^{-2} K^{-2})	Internal resistance (MΩ)	Thermal resistance (K/W)
Al/n-poly-Si	93.7	7.46	3.63×10^{-3}	0.383	1.555
p-$Bi_{0.5}Sb_{1.5}Te_3$/n-$Bi_{0.87}Sb_{0.13}$	95.8	23.8	8.14×10^{-3}	1.73	2.127

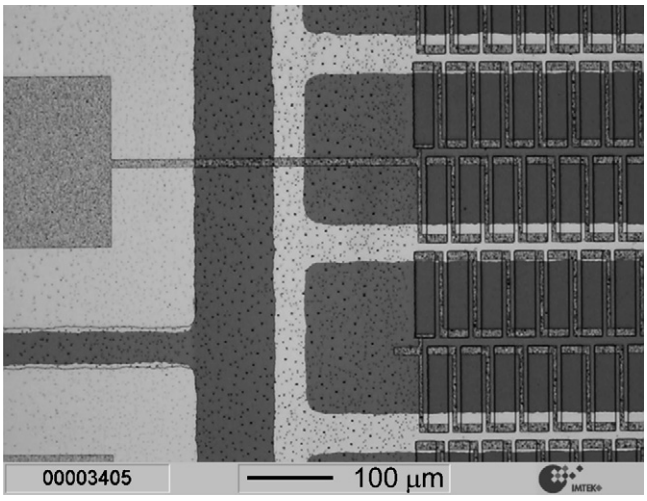

Fig. 5. Microscope image of the in-plane thermocouples during the fabrication process. The light areas indicate the starting layer for the electrochemical deposition of the gold layer contacting the hot end of the thermocouples.

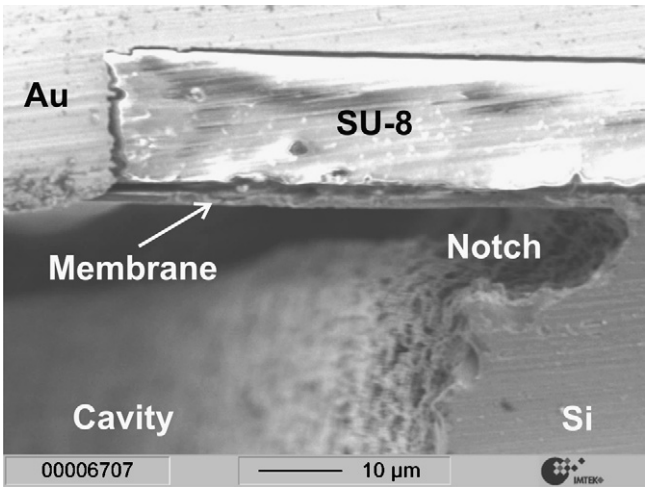

Fig. 7. SEM image of a cut through the chip with a detail of the thermoelectric membrane.

Fig. 4). To establish the electrical contact between the Al and poly-Si, the wafer is tempered for 60 min at 450 °C. Finally, the thermocouples are covered by 1.2 µm PECVD SiO_2 to electrically insulate the thermocouples from the electrodeposited gold layer. The bond pads are opened by dry etching to allow for an electrical contact.

The fabrication of Module B starts with the deposition of a Cr/Au starting layer, 20/70 nm thick, which is subsequently structured by wet etching to avoid parasitic heat losses from conduction through the film (Fig. 5). An SU-8-2010 layer (20 µm thick) is spin-coated on the start layer and structured by photolithography. The remaining SU-8 structures form trenches above one thermocouple junction, which are filled with gold by electroplating. After filling the trenches, a second Au layer is deposited on the whole wafer and structured to insulate the bond pads. This layer serves as starting ground for the second Au electroplating process, which forms the top thermal contact pad.

After the electroplating process, the backside of the 300 µm thick Si wafer is structured in Module C. The membrane is released by a DRIE process in an STS-ICP, to thermally insulate the thermoelectric structure. The DRIE process is operated with increasing platen power to yield negative angle walls and a small contact line at the thermocouple junction. Over etching further increases the membrane length as described above. The cross-section of a fabricated generator chip is displayed in Figs. 6 and 7.

Fig. 8 shows a complete generator chip with the large thermal contact area in the middle, type number, and bond pads at the left and right side. These bond pads not only allow to harvest the electric power from the entire chip, but also serve for separate measurements at each row of thermocouples.

In the first fabrication run, test structures are manufactured with n-poly-Si and Al to characterize the fabrication procedure and yielded materials. In a second run, the complete thermoelectric generators are fabricated.

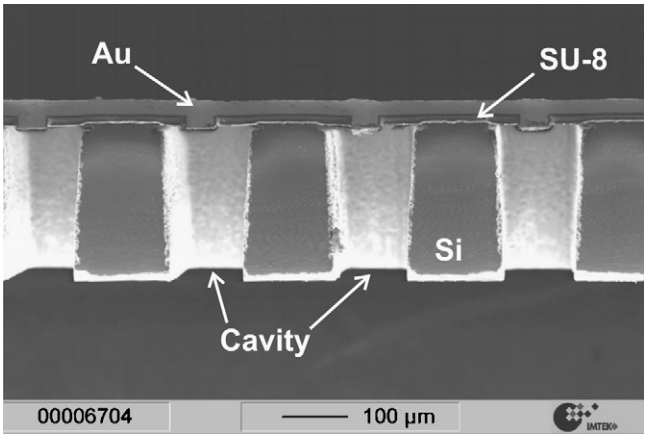

Fig. 6. SEM image of a cut through the chip.

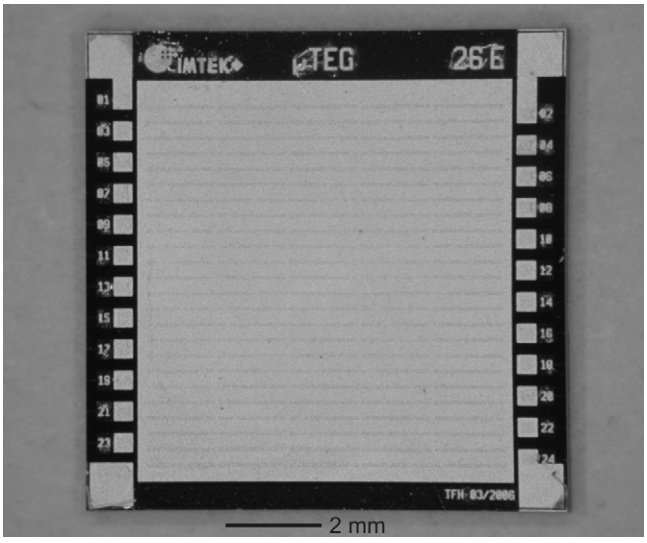

Fig. 8. Photograph of a diced chip with an area of 10 mm × 10 mm.

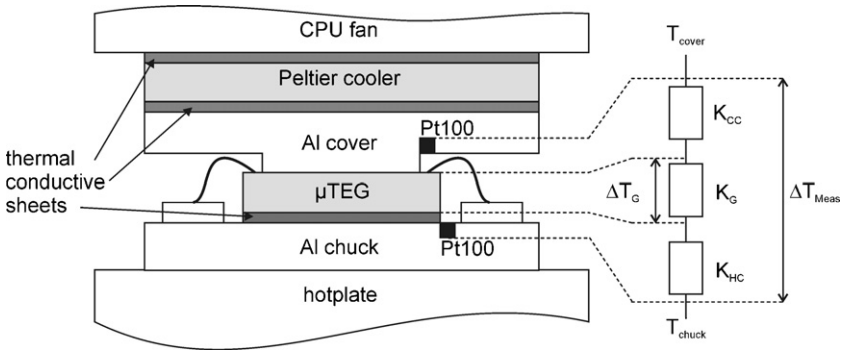

Fig. 9. Schematic of the measurement setup with a thermal network indicating the thermal contact resistances that consume approximately 85.7% of the applied temperature difference.

5. Device testing

Van-der Pauw structures are used to measure the electrical resistivity of the thermoelectric active materials. In order to determine the Seebeck coefficient, membrane-based test structures are employed. The electrical resistivity is found to be $6.294 \pm 0.204\ \mu\Omega\,m$ for n-poly-Si and $0.04303 \pm 0.111\ \mu\Omega\,m$ for Al. The measured Seebeck coefficient of the material pair n-poly-Si/Al is $106.18 \pm 4.63\ \mu V\,K^{-1}$. The values for poly-Si are in good agreement with the data found in the literature (gate poly CAE: $111.3 \pm 1.5\ \mu V\,K^{-1}$, $6.61 \pm 0.17\ \mu\Omega\,m$) [15].

For characterization of the generator devices, a measurement setup is developed, where a temperature difference is applied across the chip and the resulting output voltage is measured (see Fig. 9). After a gross function test of the fabricated structures, operable thermoelectric generators are selected and mounted on an aluminum chuck using a thermal conductive sheet. A hot plate heats the chuck. The top thermal contact is established via a pressure contact between the chip and a cover plate made of aluminum. A commercial Peltier cooler combined with a CPU fan cool the cover plate. The temperature difference is measured with PT100 resistors, which are integrated into the chuck and the cover plate. Thus, the temperature difference across the generator ΔT_G is limited due to the thermal contact resistances between the cover plate and the generator K_{CC} and between the chuck and the generator K_{HC}. According to the data sheet the contact resistance K_{HC} of the thermal conductive sheet is approximately $0.5\ K\,W^{-1}$. Literature data for the thermal contact resistance of an Al/Al pressure contact enable a rough estimation for K_{CC} of approximately $8.8\ K\,W^{-1}$ [16]. As described in the simulation section, the thermal resistance of the generator K_G is $1.555\ K\,W^{-1}$. Thus, the temperature difference across the chip ΔT_G is reduced to 14.3% of the externally measured value ΔT_{Meas}.

Wire bonding is used to electrically connect the chips to the measurement equipment. A Keithley 2700 digital multimeter with a Keithley 7700 multiplexing card registers the output voltage and temperature difference.

Fig. 10 depicts the measured open-circuit voltage of 125 thermocouples as a function of the temperature difference across the device. The open-circuit voltage depends linearly with $9.51\ mV\,K^{-1}$ on the temperature difference between the bottom and the top side of the chip.

The internal resistance of the 125 thermocouples under test was measured to 84 kΩ, which would result in 5.04 MΩ for the entire device with 7500 thermocouples, compared to a simulated value of 0.383 MΩ. This difference results from high contact resistances and inhomogeneous Al layers. The Al layer of the device was slightly porous and showed over etchings (mousebites) from wet etching resulting in uncertainties concerning the electrical resistance of the thermocouple meander.

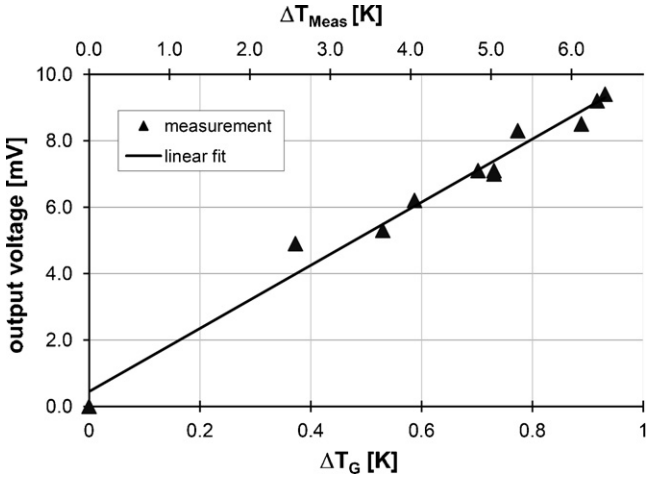

Fig. 10. Measured open-circuit voltage of a demonstrator device with 125 thermocouples. The upper scale indicates the measured temperature difference between the chuck and cover. The lower scale displays the calculated temperature difference across the chip.

6. Discussion

From the measured open-circuit voltage a device power factor of $1.612 \times 10^{-4}\ \mu W\,mm^{-2}\,K^{-2}$ can be extrapolated. This value is one order of magnitude lower than the simulated value of $3.63 \times 10^{-3}\ \mu W\,mm^{-2}\,K^{-2}$. The major source for this deviation is the increased electrical resistance of the device due to problems in Al processing.

Infineon has developed comparable thermoelectric generators with 15,782 thermocouples of n- and p-poly-Si on an area of $7\ mm^2$. These generators have a high internal resistance of 2.1 MΩ and a power factor of $4.26 \times 10^{-4}\ \mu W\,mm^{-2}\,K^{-2}$ [9]. Thermoelectric generators developed and fabricated by HSG-

IMIT and Kundo deliver a power of 1.5 μW from a temperature difference of 10 K on a chip size of 16.5 mm^2 [8]. Using these data, a power factor of 9.1×10^{-4} $\mu W\,mm^{-2}\,K^{-2}$ is calculated.

For their thick-film-based generator with a chip size of 1.12 mm^2, Micropelt reports an output power of 0.67 μW with a temperature difference of 5 K applied [4]. This gives a power factor of 2.4×10^{-2} $\mu W\,mm^{-2}\,K^{-2}$.

The simulated power factors of 3.63×10^{-3} $\mu W\,mm^{-2}\,K^{-2}$ for the Al/n-poly-Si generator and 8.14×10^{-3} $\mu W\,mm^{-2}\,K^{-2}$ for the BiSbTe-based generator exceed those of previously presented thin-film-based devices. Yet, thick-film-based thermoelectric generators show power factors that are one order of magnitude higher. At the current state it is doubtful whether thin-film-based devices can challenge the superior power factors provided by thick-film devices due to their inherently high internal electrical resistance. However, an output power in the μW range is of increasing interest for the supply of ultra-low power CMOS electronics, which would allow the combination of μ-TEGs with distributed and embedded microsystems.

Also, concerning the output voltage per area, thin-film devices with a higher integration density are favorable. The device presented in this work theoretically produces an output voltage per area of 7.46 $mV\,mm^{-2}\,K^{-1}$ (Al/n-poly-Si) and 23.8 $mV\,mm^{-2}\,K^{-1}$ (BiTe) compared to 0.87546 $mV\,mm^{-2}\,K^{-1}$ (calculated using data given in [4,6]) generated by the Micropelt device. This shows the potential of the proposed thermoelectric generator concept.

7. Conclusion

In this work a novel way of manufacturing a thin-film-based thermoelectric generator is proposed. The fabrication process is segmented into three modules. The first module concerns the thermoelectric structure, which is deposited in thin-film technology. The second and third modules include the heat conductive structures that are necessary to yield a high in-plane temperature gradient, while the heat flux is perpendicular (cross-plane) through the device. That way, the thermal contact areas are maximized while at the same time achieving a high integration density of thermocouples. The modular approach allows to fabricate thermopiles in any material system, that is compatible with silicon technology. The thermoelectric setup enables not only the power supply of autonomous devices, but can also directly be used as sensor for heat flux or temperature difference. In both cases the boundary conditions must be known and kept constant for the measurement setup. Devices with thermocouples made of Al and n-doped poly-silicon, as well as p-$Bi_{0.5}Sb_{1.5}Te_3$ and n-$Bi_{0.87}Sb_{0.13}$, are modeled. Simulation results indicate similar performance to other existing thin-film-based devices. A prototype generator is designed and fabricated using the in-house clean-room facilities. An output voltage of 9.51 $mV\,K^{-1}$ is determined, proofing the feasibility of the concept.

References

[1] A.F. Joffe, The revival of thermoelectricity, Sci. Am. 199 (1958) 31–37.
[2] D.M. Rowe (Ed.), Handbook of Thermoelectrics, CRC, London, 1995.
[3] M. Kishi, H. Nemoto, M. Yamamoto, S. Sudou, M. Mandai, S. Yamamoto, Microthermoelectric modules and their application to wrist-watches as an energy source, in: Proc. IEEE, 18th ICT, 1999, pp. 301–307.
[4] H. Böttner, J. Nurnus, A. Gavrikov, G. Kühner, M. Jägle, C. Künzel, D. Eberhard, G. Plescher, A. Schubert, K.H. Schlereth, New thermoelectric components using microsystem technologies, J. MEMS 13 (2004) 414–420.
[5] G.J. Snyder, J.R. Lim, C.K. Huang, J.P. Fleurial, Thermoelectric microdevice fabricated by a MEMS-like electrochemical process, Nat. Mater. 2 (2003) 528–531.
[6] W. Glatz, S. Muntwyler, C. Hierold, Optimization and fabrication of thick flexible polymer-based microthermoelectric generator, Sens. Actuators A 132 (2006) 337–345.
[7] F. Völklein, Thermal-based microsensors, in: MEMS—A Practical Guide to Design, Analysis and Application, William Andrew, 2006 (Chapter 5).
[8] H. Glosch, M. Ashauer, U. Pfeiffer, W. Lang, A thermoelectric converter for energy supply, Sens. Actuators 74 (1999) 246–250.
[9] M. Strasser, BT Entwicklung und Charakterisierung Mikrostrukturierter Thermoelektrischer Generatoren in Silizium-Halbleitertechnologie, PN Shaker Verlag (2004), ISBN 3-8322-3420-9.
[10] Z. Wang, V. Leonov, P. Fiorini, C. Van Hoof, Micromachined thermopiles for energy scavenging on human body, in: Proc. IEEE, 14th Transducers, 2007, pp. 911–914.
[11] H. Böttner, G. Chen, R. Venkatasububramanian, Aspects of thin-film superlattice thermoelectric materials, devices, and applications, MRS Bull. 31 (2006) 211–217.
[12] G.S. Nolas, J. Sharp, H.J. Goldsmid, Thermoelectrics—Basic Principles and New Material Developments, Springer, Berlin, 2001.
[13] G. Kalitzin, Thermodynamik Irreversibler Prozesse, VEB Deutscher Verlag der Grundstoffindustrie, Leipzig, 1968.
[14] G. Kluge, G. Neugebauer, Grundlagen der Thermodynamik, Spektrum Akademischer Verlag, Heidelberg, 1994.
[15] O. Paul, P. Ruther, Material characterization, in: CMOS-MEMS, Wiley–VCH, 2005 (Chapter 2).
[16] R.R. Tummala, E.J. Rymaszewski, A.G. Klopfenstein, Microelectronics Packaging Handbook, Part I, Chapman & Hall, 1997.

Biographies

Till Huesgen is a PhD student at the Laboratory for Design of Microsystems, Department of Microsystems Engineering-IMTEK, University of Freiburg, Germany. From 2000 to 2006, he studied microsystems engineering at the University of Freiburg and received his diploma degree with a focus on the design and fabrication of thermoelectric generators. He is currently working for the graduate programme "Micro-Energy Harvesting" on thermo-mechanical energy conversion.

Peter Woias is a full professor at the Laboratory for Design of Microsystems, Department of Microsystems Engineering-IMTEK at the University of Freiburg, Germany. After studying electrical engineering from 1982 to 1988, he received his PhD in 1995 from the Technical University in Munich, Institute of Integrated Circuits. Later on he worked at the Fraunhofer Research Institute in Munich as a group leader on microfluidics. In 2000, he became a full professor in Freiburg, where he enlarged his research interest to micro-rapid prototyping, mechanical actuators, CAD and simulation in microsystem design.

Norbert Kockmann is a scientific group leader at the Laboratory for Design of Microsystems, Department of Microsystems Engineering-IMTEK, University of Freiburg, Germany. His research activities are in microprocess engineering and transport phenomena in microsystems. He received his diploma degree from the Technical University of Munich and finished his PhD in 1996 at the University of Bremen, Technical Thermodynamics, Heat and Mass Transfer. After 5 years of industrial experience as a project manager for design and construction of chemical plants, he joined the University of Freiburg in 2001 and works now on several research projects on heat and mass transfer, coupled transport phenomena, mixing, and chemical reactions in microchannels.